arXiv:astro-ph/9905093v1 7 May 1999

Introduction to Unified Schemes

Beverley J. Wills

McDonald Observatory & Astronomy Department, University of Texas at Austin, TX 78712, USA

Abstract.

The differences among apparently diverse classes of AGN are mainly the result of viewing the central engine at different orientations, because dust, which absorbs and scatters the light, partially covers the central source, and because synchrotron emission is highly beamed along the relativistic jet. Also important are factors independent of orientation: the total power output, the unknown mover behind the eigenvector 1 relationships, and the radio-loudness. These other factors may not be independent of the parameters of Unified models, such as intrinsic jet physics, AGN dust content, and torus thickness. We outline the basic evidence for orientation Unified Schemes, and briefly discuss their importance for understanding the mechanisms of the central engine and its relation to the surrounding host galaxy and beyond.

1. Introduction

There is a bewildering array of AGN classes. Surprisingly, it's only in the last few years that we've realized that much of this diversity is simply the result of viewing an axisymmetric central structure from different angles. Synchrotron emission from the relativistic jets is much brighter when viewed along the jet direction (the central engine's axis), and a torus of dust obscures a low-latitude view of the center. While the real physics is buried in the center, along with clues to the enormous range of AGN luminosities, the mysterious cause of strong relationships among X-ray continuum and emission lines[1] and the apparent radio-loud–radio-quiet dichotomy, 'orientation' Unification Schemes are not simply geometrical complications, but lead us to new ways of probing the central engine and its interaction with the surrounding space. This overview will emphasize QSOs, the highest luminosity AGN. First, and most importantly, we discuss the unification of radio-loud AGN (§2). This is of prime importance because the axis of the central engine can be defined by the innermost radio jets. The strongest arguments for unification (axisymmetry) of properties at IR through X-ray wavebands can be made when observational properties can be referred to this axis, even for radio-weak (radio-quiet) AGN. In §3, we present an idealized

[1] The so-called Eigenvector 1 or Principal Component 1 relationships link X-ray continuum slope, linewidths and the strengths of Fe II emission and other lines (Wills et al. & Francis & Wills contributions, this volume.)

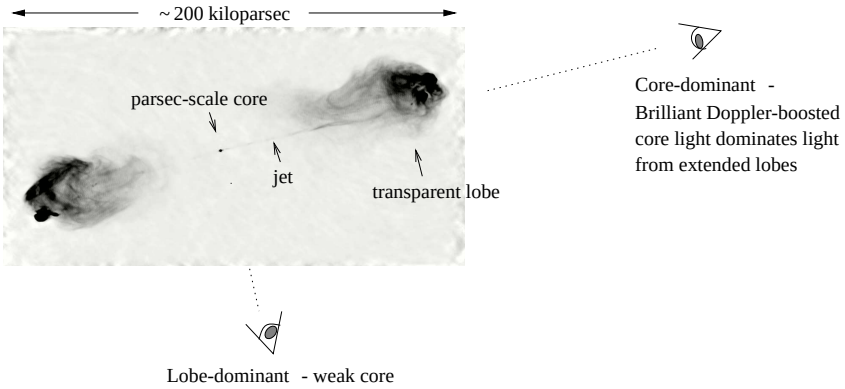

Figure 1. Radio source unified scheme. The observer below the figure views the radio source almost perpendicular to the jet directions. This observer sees strong, clearly separated lobes, a weak unresolved core coincident with the optical galaxy, and faint unresolved jets linking the core to the lobes. The central AGN is hidden from this observer both by dust in the plane of the galaxy, and a dusty torus whose axis lies close to the jet. The observer to the right views the center from a direction close to the jet axis. The relativistic jet beams Doppler-boosted synchrotron radiation along the jet axis, so this observer sees a brilliant, time-variable radio core with the lobes now seen as a relatively very faint elongated halo. The image is a real one, actually that of Cygnus A, mapped at 6 cm with NRAO's Very Large Array with $0.5''$resolution, viewed nearly perpendicular to the jets. (courtesy, Chris Carilli – http://mamacass.ucsd.edu:8080/people/pblanco/cyga6cm_small.gif).

picture that unifies a wealth of IR through X-ray properties, relating these to the radio axis. Arguments in support of the general dusty torus picture are provided by a few specific examples (§4) and by some statistical arguments (§5). An overview and speculations are given in §6. Additional references are given in §7. More detailed reviews are given by Antonucci (1993) and, for radio-loud AGN, by Urry & Padovani (1995).

2. Radio-loud AGN Unification

The first recognized clues to unification came from the structure of radio sources because they can be spatially resolved, even on parsec scales for nearby AGN. Extragalactic radio sources often show double lobes separated by tens to hundreds of kpc, straddling a weak compact 'core' coinciding with an optical galaxy or QSO (Fig. 1). The emission mechanism is synchrotron radiation. The lobes have steep radio spectra ($F_\nu \propto \nu^{-\alpha}$, $\alpha \sim 1$) so these lobe-dominated (LD) sources are most often selected by surveys at low radio frequencies; the cores generally have flat radio spectra, the superposition of several peaked spectra from optically thick sub-components. In high-frequency radio surveys many compact, flat-spectrum sources have been discovered, often unresolved on kpc scales (the core-dominated or CD sources), usually identified optically with QSOs, occa-

sionally with their almost lineless counterparts, the BL Lac objects. The first clue to relativistically-beamed synchrotron emission came from the intensely bright, highly variable radio cores of these BL Lac objects and the Optically Violently Variable (OVV) QSOs, with light travel sizes of light-hours implying impossibly high brightness temperatures – exceeding the Compton scattering limit. The second clue came from Very Long Baseline Interferometry (VLBI) that probed the compact radio sources on scales of milliarcseconds. Blobs were ejected, apparently at superluminal speeds in the plane of the sky. As blobs travel towards the observer at relativistic speeds, $\gtrsim$0.7c, the emitted signal has less far to travel, that is, the blobs tend to 'catch up' with their forward-emitted radiation; thus, for a distant observer looking close to the direction of ejection, events appear to happen closer together in time, and the blob appears to travel at speeds up to 10c or more. Under these conditions, the synchrotron radiation will be forward-boosted into an angle γ^{-1} rad,[2] and with amplification or Doppler boosting up to a factor $\delta^{n+\alpha}$ (n = 2 – 3), simultaneously explaining the brilliant compact sources. The most general Unification Scheme for radio sources states that all CD sources are LD sources viewed close to the jet axis (within 15°–20° of the line of sight.) This is illustrated in Fig. 1.

For a random distribution of orientation angles one expects to see $\sim 2\gamma^2$ LD sources for every CD source. This is more-or-less consistent with the statistics of radio sources, taking into account the frequency and flux-density limits of radio surveys (Urry & Padovani 1995). This is nice, but somewhat unexpected in the sense that it is not obvious why the electrons producing the Doppler-boosted emission should have same γ as the flow pattern determined from apparent superluminal motion: first, the boosted radiation is dominated by those electrons that happen to be traveling in the observer's direction, so a spread in direction of the electron stream could result in an actual beam width much broader than γ^{-1} (Lind & Blandford 1985). Second, the pattern speed is probably an apparent speed, representing the phase velocity of shock fronts in the jet. Several observations suggest that the pattern speed is in fact close to the speed of the Doppler-boosting electrons, so we're in luck.

The optically-thin emission from the lobes is isotropic, so what this means is that we have a measure of orientation of the central engine (or inner jet), the core dominance, defined by:

R = observed core flux-density/unbeamed lobe flux-density

converted to rest-frame frequencies, often chosen as 5 GHz.

This Unified Scheme predicted the following:

• The jets should have very different brightnesses. The approaching jet should be brighter than the receding jet, by $[(1+\beta\cos\theta)/(1-\beta\cos\theta)]^{n+\alpha}$. In fact the fainter jet is rather faint even when it's thought that the jets are close to the sky plane. These jet asymmetries are observed out to several Kpc (in powerful 3CR sources, at least). The lobes are of similar brightnesses to each other because by the time the jet has reached them it has become much less relativistic, and environmental factors can dominate (Bridle et al. 1994; Dennett-Thorpe et al. 1997; Wardle & Aaron 1997).

---

[2] The Lorentz factor $\gamma = (1-\beta^2)^{-1/2}$, and the Doppler factor $\delta = \gamma^{-1}(1-\beta\cos\theta)^{-1}$.

• The brighter jet is on the near side of the nucleus. This is beautifully demonstrated by radio Faraday depolarization which is almost always greater for lobe emission on the side of the fainter (invisible) jet. Recent observations have shown that the depolarization occurs in a foreground screen associated with the radio source, rather than being intrinsic to the lobes, so overcoming an earlier objection to this argument (e.g., Leahy et al. 1997; Morganti et al. 1997).
• Slight curvature of jets, when foreshortened as expected in CD sources, should appear to be much larger than in LD sources. This is observed (Hough & Readhead 1989; Cohen & Unwin 1982.)
• Core-dominated sources, whose apparent brightness often exceeds the Compton limit, should be seen as strong emitters of X-rays and γ-rays, a prediction strikingly confirmed (Urry 1999).
• Apparent superluminal speeds should decrease with decreasing core dominance, and this is observed (Browne 1987; Vermeulen & Cohen 1994).
• The CD sources have relatively faint diffuse halos with structure, often double, and luminosity consistent with their being the extended doubles seen end-on. On this basis Antonucci & Ulvestad (1985) used the converse to argue that the radio source Unified Scheme must be basically correct: CD sources seen at larger angles to the jet must be seen as powerful steep spectrum radio sources dominated by extended, basically double-structured emission, and can account for most of the fraction of observed LD sources.
• There is an inverse relationship between R and projected linear size. Barthel (1989) showed that the projected (apparent) radio linear sizes for 3CRR QSOs are smaller than for the lower-R FR II radio galaxies, as predicted. A quantitative demonstration of this relationship has been thwarted by selection effects and probable linear size evolution (Gopal-Krishna et al. 1996; Neeser et al. 1995).

While many radio sources show clear double-lobed structure (e.g., Fig. 1), in real life structure can be more complex on both parsec and kiloparsec scales. About 20% of sources in low radio-frequency surveys consist of intrinsically compact double or single sources – Gigahertz Peak Spectrum (GPS) and Compact Steep Spectrum (CSS) sources (Urry & Padovani 1995). It is not yet clear whether unification works for these intrinsically compact sources. Also, the LD sources come in two flavors, FR I and FR II (Fanaroff & Riley 1974; Owen et al. 1996). The lobes of the more luminous[3] FR II sources contain bright hotspots and are edge-brightened where they ram into the surrounding medium, whereas the less luminous FR I lobes are relaxed and show neither of these features.

3. Unification of the Optical, Infrared and X-ray Properties

The central regions of luminous AGN are essentially unresolved at non-radio wavelengths, and their classification is based on optical spectra.

Optical spectra of Type 1 are defined by their broad emission lines (~ 6000 km/s FWHM), which originate in gas within 1 pc of a central supermassive black hole. They may also show narrow lines that arise from low density gas on scales of parsecs to kiloparsecs. Type 1 spectra are accompanied by a broad

[3] $L_\nu(178\mathrm{MHz}) \gtrsim 1.3 \times 10^{33}$ erg s^{-1} Hz^{-1}, for H$_o$ = 50 km s^{-1} Mpc^{-1}.

optical-EUV bump attributed to thermal emission with a range of temperatures, 10^4 K to 10^5 K, arising from an accretion disk that feeds the black hole (Shields 1978; Malkan & Sargeant 1983; Mushotzsky 1997). These observed properties define the QSOs and their lower-luminosity cousins, the Seyfert 1 nuclei. Optical surveys for these objects usually depend on selection by blue or UV colors and strong broad emission lines. In radio-loud AGNs it appears that Type 1 spectra are found in FR II radio sources, but almost never in the lower luminosity FR Is (Falcke et al. 1995).

Optical spectra of Type 2 are those seen to have narrow lines only, with a spectrum and velocity dispersion indistinguishable from the narrow lines of Type 1 spectra. The optical continuum is dominated by starlight, and there is no convincing evidence for a optical-EUV bump associated with narrow line spectra.

When seen in the abscence of obscuration, the thermal Type 1 and Type 2 emission lines and optical-EUV bump are essentially unpolarized.

In core-dominant radio-loud AGNs a steep-spectrum, polarized, smooth spectral energy distribution of an IR-optical-UV synchrotron component can contribute (the blazars), in some cases overwhelming the emission lines and accretion continuum of a Type 1 spectrum. The spectra of BL Lac objects often appear featureless, and are always dominated by this synchrotron continuum, and may have no, or intrinsically only very weak broad lines. Narrow emission and absorption lines may be present, as for any AGN.

Fig. 2 illustrates how AGN can appear drastically different at different orientations. It shows (not to scale) a cross section through the dusty torus, whose shadow is shown in gray. A radio jet axis is shown aligned with the axis of the dusty torus. The broad lines arise from dense gas of the broad-line region (BLR) and narrow emission lines from less-dense NLR gas. These are shown as filled and open circles in Fig. 2. Refer to Fig. 2 in the remainder of this section.

3.1. Powerful FR II Radio-Loud (RL) AGNs.

One can see the BLR and accretion continuum directly from within the cone whose edge is defined by the shadow of the torus. Within 15° to 25° of the jet axis the QSOs are CD with $R \gtrsim 1$, and the strong variable synchrotron emission is revealed by a steep polarized infrared-UV continuum that may swamp the unpolarized blue bump and emission lines. These QSOs are therefore often seen as optically violent variable (OVV) or highly-polarized (variable) QSOs (HPQs). Beamed Compton-scattered radiation from the jet contributes to and flattens the X-ray spectrum.

At larger angles to the axis the QSOs are LD ($R \lesssim 1$), and the beamed synchrotron emission is no longer detectable against the optical-EUV bump. The broad Hβ line and broad base of the C IVλ1549 emission lines are broader than in CD QSOs, perhaps indicating a disk-like configuration for the inner BLR.

At even larger inclinations of the jet axis, perhaps 40° to 50°, R decreases further, with increasing projected lobe separations (Barthel 1989). Broad lines may be very broad, up to 10,000 or even 20,000 km s^{-1} in Doppler width (FWHM), and are usually reddened and weaker relative to the NLR emission (Grandi & Osterbrock 1978; Hill, Goodrich & DePoy 1996). Some of these

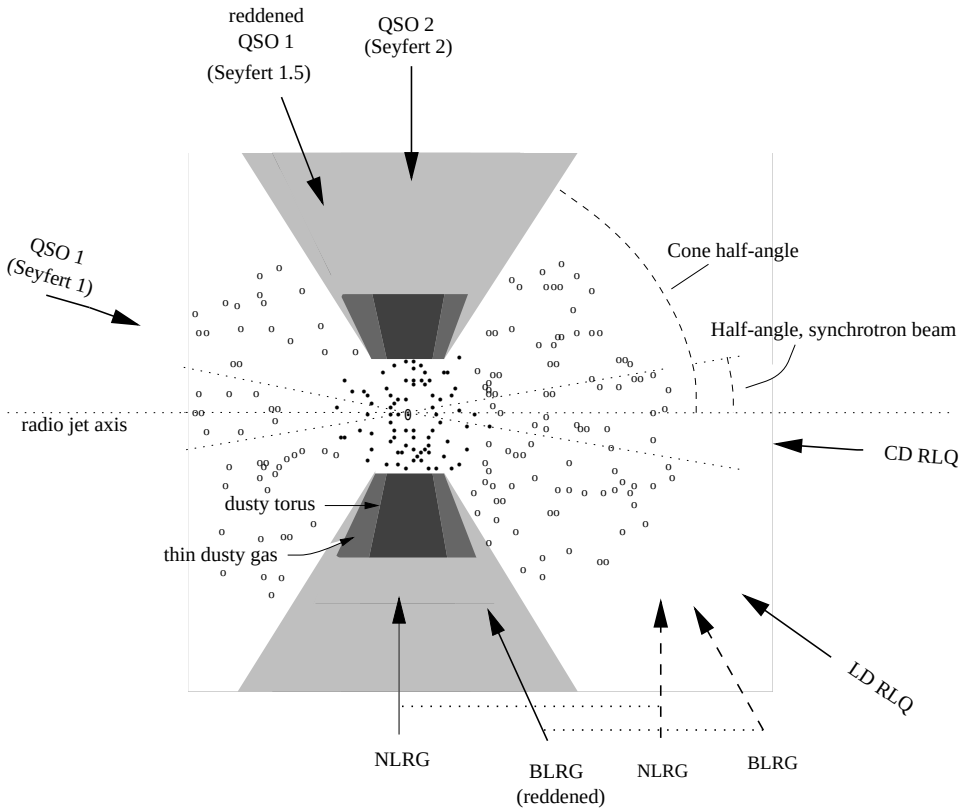

Figure 2. A similar central engine viewed from different inclinations to the axis gives rise to different classes of AGN. Dense, high speed ($\sim 7000\,\mathrm{km/s}$) gas of the BLR (solid dots) may be exposed to view, partially absorbed, or completely hidden by the dusty torus (shadow shown in grey). The dashed arrows show directions from which a polarized, scattered light spectrum of the center can arise. At least half of the lower-velocity NLR gas (open circles) is seen from any view, except the highest ionization NLR close to the center. Imagine you, the observer, are situated at very great distances so that, e.g., the two views of a NLRG are seen in parallel light, as indicated. Left and top of the diagram are radio-quiet (RQ) classifications, and right and bottom are radio-loud (RL) classifications.

reddened QSOs and broad-lined radio galaxies (BLRG) show weak, polarized broad-line and continuum spectra — evidence for a scattered Type I spectrum that is combined with the reddened view through the thinner regions of the torus.

At even larger inclinations emission from the NLR completely dominates the spectrum (Fig. 3). These are the narrow-lined radio galaxies (NLRG) with their Type 2 spectra. Direct light from the BLR and optical-EUV continuum may be completely obscured, and even the higher-ionization NLR emission ([O III]λ5007) may be partially obscured by the dusty torus. Starlight completely dominates the near IR-optical continuum. The inner regions may be seen indirectly however, as a faint polarized spectrum that has been scattered from within the opening angle of the torus – the 'ionization cone' or 'scattering cone'. Even the scattered light may be absorbed as it grazes the torus – or passes through the host galaxy. These ionization cones are sometimes resolved by HST and ground-based imaging.

The "3μm Bump" arises from warm dust near evaporation temperature ($\sim$ 1700 K). This equilibrium temperature determines the distance of the inner torus from the central heat source, $\sim L_{46}^{1/2}$ pc for luminous QSOs of bolometric luminosity $L_{46} \times 10^{46}$ ergs s^{-1}. This is present in most, if not all, RL QSOs (RLQs).

3.2. FR 1 AGN and BL Lac Objects

Does the above Unified Scheme also hold for the FR I AGN, which are less luminous? Most FR I AGN are LD sources and appear optically as radio galaxies. No FR I radio galaxy had shown anything but weak narrow line emission until recently, when Lara et al. (1998) discovered an FR I nucleus with broad emission lines. The BL Lacs, which are always CD, are probably the LD FR I radio galaxies seen at small angles to the radio jet. Consistent with this, is their lack of, or only very weak, broad emission lines. The extended radio fuzz around BL Lac cores is consistent in luminosity and structure, and probably in size as well, with the extended radio emission of double-lobed FR I radio galaxies. The evidence for relativistic jets in BL Lac objects has already been mentioned: (i) from their high apparent brightness temperature and rapid variability. Their radio-IR-optical-UV continua are smoothly connected, linearly polarized and highly variable, as expected for a beamed synchrotron origin. The BL Lacs are so far the only AGN detected at TeV (γ-ray) photon energies – attributable to beamed radiation from the relativistic jet, and their lower redshifts (smaller distances) than most core-dominant RLQs. (ii) The jets are also seen in VLBI images. While the extended lobes of FR I radio galaxies are relaxed, with no edge brightening or hotspots, their inner radio jets are indistinguishable from those of FR II sources, and apparent superluminal motion has been measured (Giovannini et al. 1998).

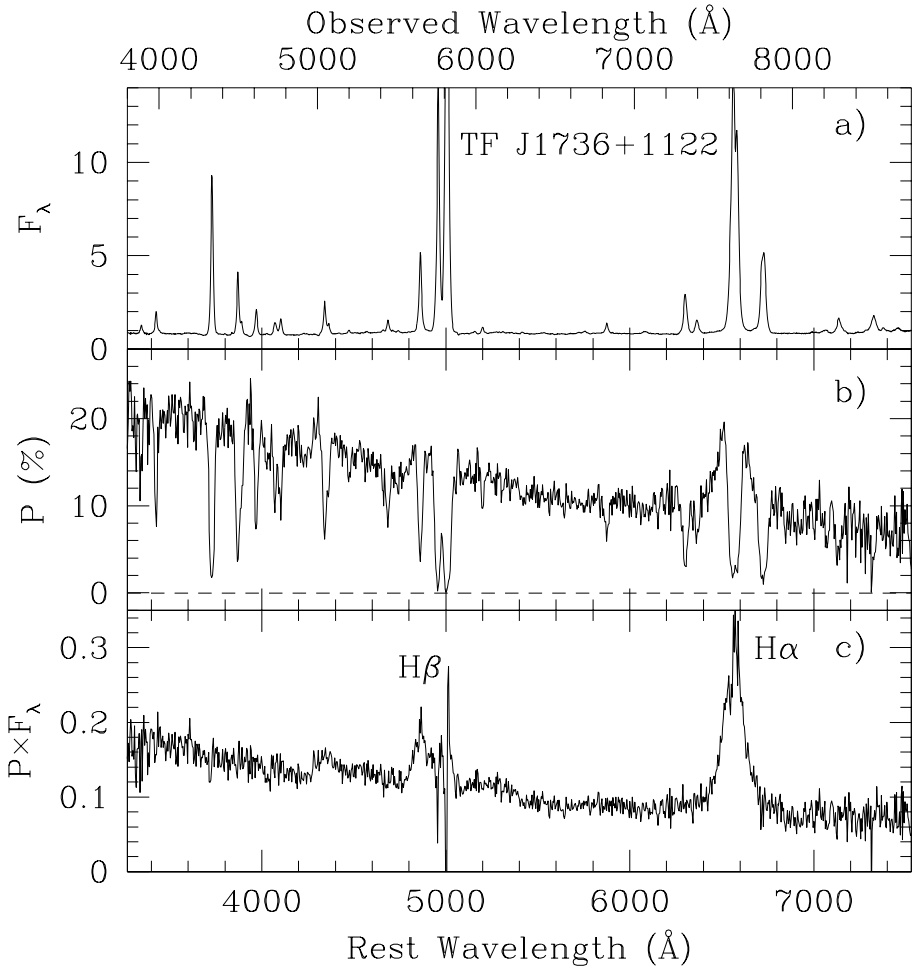

Figure 3. Spectropolarimetry of the QSO 2 TF J1736+1122. The upper panel shows the spectrum in total (polarized plus unpolarized) light, dominated by the , strong NLR emission characteristic of a Type 2 spectrum. The spectrum in the middle panel shows the degree of polarization. Note how the degree of polarization drops at the wavelengths of the strong, essentially unpolarized, QSO 2 narrow lines. The lower panel shows how the faint scattered-light QSO 1 spectrum is revealed in polarized light. Note the broad, blended Fe II emission peaking near 4570Å and 5250Å, and the broad Balmer lines in the polarized flux spectrum. (Figure from Tran et al. 1999).

3.3. Radio Quiet (RQ) AGN

Radio-quiet (RQ) AGN include both the RQ QSOs (RQQs), which are of course optically luminous, and the Seyfert galaxies, which are less luminous[4]. Their radio emission is weak, though detectable.

For nearby Seyfert 1s and 2s, ionization-scattering cones can be related to their radio jet axes, and their unification by orientation is quite well established both statistically, and for many individual Seyfert 2s where a buried Seyfert 1 has been revealed in polarized light (§4 & §5). This does not preclude the existence of a small fraction of genuine Seyfert 2s where the BLR is intrinsically weak, perhaps temporarily (e.g., N4151, Penston & Perez 1984).

Does this unified scheme hold for radio-quiet QSOs? Kukula et al. (1998) argue that the radio-quiet QSOs form the high radio and optical luminosity extension of the Seyfert 1 luminosity functions, which is suggestive that it does. While it has been shown that there is patchy covering by absorbing and scattering dust in radio-quiet QSOs (§6), the dust geometry has not been clearly related to the axis of the central engine. Also, no large, unbiased survey has been made for QSO 2s – whatever they may be expected to look like.

Radio-quiet QSOs & the Axis of the Central Engine The QSO radio luminosity function appears bimodal (Hooper et al. 1995) so a distinction has been made between radio-loud QSOs (RLQ) and radio-quiet QSOs (RQQ). A somewhat arbitrary definition often used to discriminate RQQ from RLQ is that RQQ have a rest-frame flux-density ratio $F_\nu(5\ \mathrm{GHz})/F_\nu(\mathrm{B\text{-}band}) \lesssim 10$. Results from deep radio surveys (*FIRST*, White et al. 1999 preprint) will show whether RQQ and RLQ are really separate populations; the lower the survey frequency the better, to avoid the complications of beamed radio emission. Recent surveys of the radio properties of radio-quiet QSOs (e.g., Falcke, Wilson, & Ho 1997; Kukula et al. 1998; Blundell & Beasley 1998a; Kellermann et al. 1994, 1998) show strong evidence for jet-producing central engines in many. Falcke et al. (1996a, b) make a strong case that a few QSOs with radio flux densities intermediate between radio quiet and radio loud are naturally explained as Doppler-boosted radio-quiet QSOs, the radio-quiet equivalent of CD RLQs. For these they derived similar γ(Doppler boosting). This is supported by the discovery of superluminal motion in at least one radio-quiet QSO (Blundell & Beasley 1998b). These new results are important for the interpretation of optical properties in terms of an axisymmetric central engine. However, it must be appreciated that only the least radio quiet of the radio-quiet QSOs can be investigated for jet structure and superluminal motion.

Broad Absorption Line QSOs An important subclass of QSOs are the broad absorption line QSOs (BAL QSOs). These objects show broad absorption features, blueshifted from a few thousand km s^{-1} up to 45,000 km s^{-1} or even more, from the systemic redshift. The observed radial terminal velocity of these BALs

[4] We reserve the term 'Seyfert' for low-luminosity radio-quiet AGN. Spectroscopically, the Seyfert 2 AGN are the radio-quiet equivalents of the low-radio-power NLRG. There appear to be no high radio-power equivalents of the Seyfert class. Apparently the production of FR II radio sources requires the presence of a powerful optical central engine, as indicated by a QSO.

is strongly anticorrelated with radio power (Weymann 1997). The soft X-rays are completely absorbed in these objects (Green & Mathur 1996). These absorption features provide evidence for high-ionization and dusty, low-ionization nuclear outflows (see §4 below). Three main results have led to the idea that all RQQs have BAL outflows:
(i) In individual BAL QSOs, from the limits on scattered light in the deep troughs, one can deduce that the absorbing gas covers ∼10% of the central continuum.
(ii) The BAL QSOs and the non-BAL QSOs have very similar UV emission line spectra (Weymann et al. 1991).
(iii) BALs are observed in ∼10% of all RQQs.
Can this 'orientation unification scheme' be related to the above scheme for radio-loud QSOs? Unfortunately, most radio-quiet BAL QSOs have only weak, unresolved radio emission, too weak for present observations at milliarcsecond (VLBI) resolutions. So no jet axis can be determined. Nevertheless, the radio structure of radio-loud BAL QSOs may soon provide important clues to orientation and radio-loud–radio-quiet differences. There may be other clues to axisymmetry and inclination, however. The BAL QSOs were the first objects as a class to show significant optical linear polarization – not counting the highly variable blazars whose high polarization arises from beamed synchrotron-emitting jets. Spectropolarimetry of several BAL QSOs shows evidence for reddened direct views of the nucleus and multiple scattered light paths. Unlike most other 'buried' Type 1 objects, the broad emission line polarization is generally low compared with the continuum, suggesting scatterers mixed with or at distances less than the BLR. In principle, the polarization position angle, and modeling the degree of polarization, may lead to further clues to the radio-quiet QSOs' inner structure (see the discussion of IRAS 07598+6508 §4.7, Fig. 4).

Serious doubt about the above simple orientation unification of BAL QSOs and non-BAL QSOs is suggested by the probable association of strong Fe II emission and weak [O III] λ5007 (NLR) emission with the existence of BALs, that is, of 'Principal Component 1' with the existence of BALs (Boroson & Meyers 1992; Turnshek et al. 1997). Several investigations suggest a range in covering factor for BAL material, so the truth may lie in orientation, together with a range in covering factor.

4. Type 1 AGN Revealed by Scattered Light: Case Studies

By now there are many examples, so we choose a few for illustration, and give references to some others.

4.1. NGC 1068, a Radio-Quiet Hidden Seyfert 1 Galaxy

NGC 1068 is the prototypical Seyfert 2 galaxy and the prototype of Type 1 nuclei buried within a dusty torus. The following situation is similar to that illustrated in Fig. 3. Spectropolarimetry revealed a faint polarized Type 1 spectrum (Miller & Antonucci 1983). In total light the scattered Type 1 spectrum is dominated by an essentially unpolarized Type 2 spectrum, nearly 100 times stronger. The Type 1 spectrum shows wavelength-independent polarization from optical to UV wavelengths (∼16%), indicating electron scattering, and the polarization is

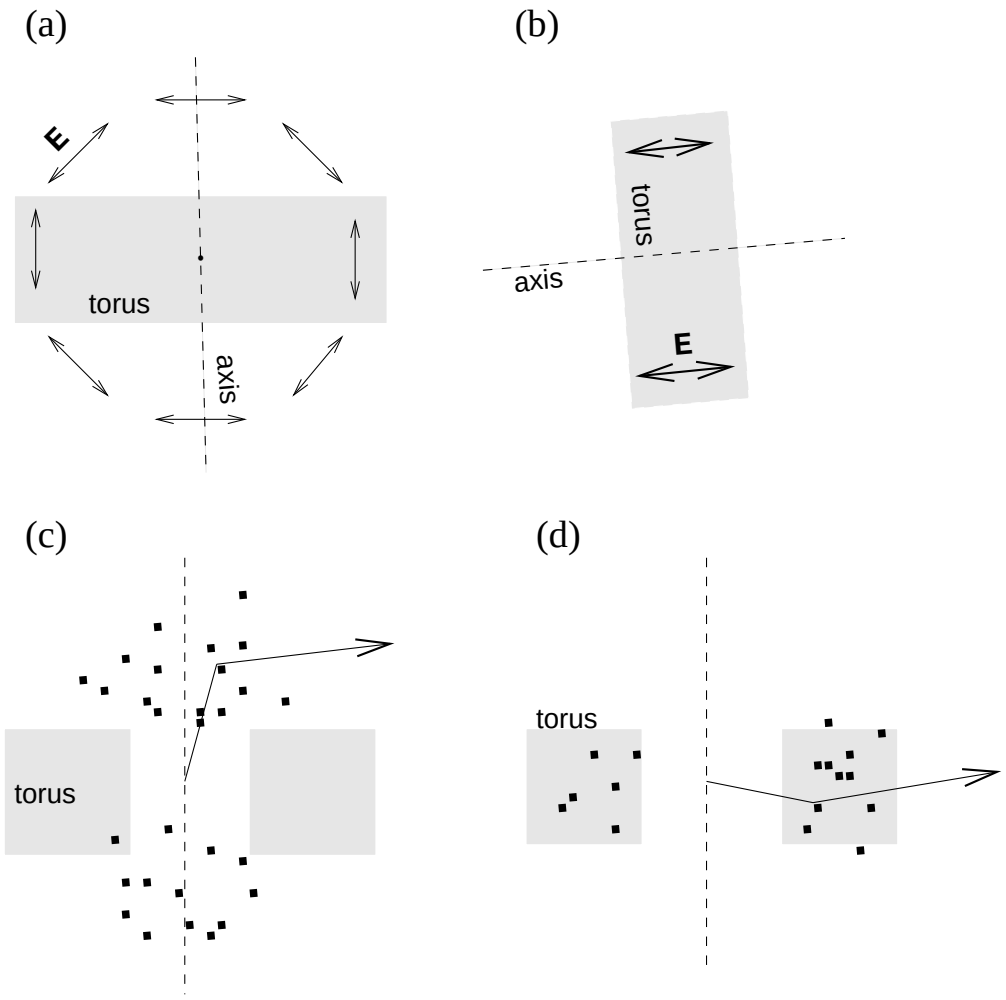

Figure 4. (a) Observer's view: Scatterers above or below optically-thick torus produce polarization **E**-vector perpendicular to the axis. (b) Observer's view: Scattering by material in an optically thin region produces **E**-vector parallel to the axis. (c) Lateral view of light path, case (a). (d) Lateral view of light path, case (b).

perpendicular to the weak radio jet (Fig. 4(a) & (c)). Direct light from the center (IR to X-rays) is obscured ($A_V \gtrsim 25^m$) by the edge-on torus, whose outer extensions have been imaged in the near infrared (on a scale of tens of pc), in thermal emission from ionized clouds on VLBA scales of ∼1 pc, and detected in H_2O and OH maser emission. Even the unresolved radio nucleus is partially absorbed. The ratio of scattered optical continuum to X-ray continuum is like that for unobscured Type 1 nuclei, indicating electron scattering of the X-ray spectrum as well. High equivalent width Fe-Kα near 6.4 keV from the unobscured scattering region was predicted and confirmed. At optical and UV wavelengths, a one-sided 'cone' of high-ionization and scattering gas, formed by the shadow of the dusty torus, subtends an opening angle of about 40° projected on the sky plane (Pogge 1988). A bicone is detected in the near infrared (Packham et al. 1997). As in many other such obscured Seyfert 1s, the ionizing photon flux seen by the emission-line gas is significantly greater than can be accounted for by our line-of-sight view of the nucleus (Wilson 1996). In fact, this was one of the first clues that the central continuum was anisotropic. In addition to the electron scattered view of the center of NGC 1068, Miller, Goodrich, & Mathews (1991) discovered a second fainter view in scattered light from a dust patch ∼ 5″NE of the nucleus. Here, a polarized Seyfert 1 flux spectrum rising to short wavelengths indicated Rayleigh-type scattering from dust grains. The dust-scattered Hβ profile from the second position shows a 'Narrow-lined Seyfert 1' spectrum, suggesting that the electron-scattered profile from the first position is broadened by thermal motion of the hot electrons.

4.2. NGC 4258, the maser galaxy

While NGC 4258 is only a very low-level AGN, it has special importance because of its closeness (∼7 Mpc) allowing good linear resolution, but especially because it contains a thin edge-on warped molecular disk, enabling the exciting discovery of water vapor maser emission. The radial velocity curve of the maser lines can be mapped at VLBI resolution, and shows a very accurate r^{-2} dependence to within 0.13 pc of the center (Miyoshi et al. 1995). This led to an estimate of $\sim 4 \times 10^7$ $M_\odot$ for the central mass, and the best evidence yet for a supermassive black hole in an active galaxy. Spectropolarimetry revealed a faint AGN-like blue continuum and emission lines polarized at 5–10%. The emission lines were broad for a low luminosity nucleus (∼1000 km s^{-1}). Polarization is perpendicular to the disk axis. These observations suggest that the molecular disk or torus obscures an AGN central engine, albeit a low-power one. High-resolution imaging in the near IR actually reveals an unresolved nucleus, suggesting A_V ∼17^m (Chary & Becklin 1997). A few additional maser sources with similar properties have since been discovered (e.g., Trotter et al. 1998).

4.3. IRAS 09104+4109, a Hidden Radio Loud FR I? QSO

This IRAS-discovered AGN is identified with a very luminous cD galaxy (z∼0.4) in a rich cooling-flow cluster. It is important because its nucleus is of QSO luminosity ($\sim 10^{12.5} h^{-2}$ $L_\odot$) and excitation, with a powerful Type 2 spectrum – a QSO 2. A scattered QSO Type 1 spectrum is seen in polarized flux (p∼20%). The radio structure is more like FR I than FR II, which makes this object of importance for both FR I and FR II unified schemes. It is one of the few 'hidden'

QSOs to show both opposed scattering-ionization cones (opening angle $\sim 46°$). These giant cones extend ~ 5 Kpc from the nucleus.

4.4. OI 287 = Q 0752+258, a LD radio-loud QSO with a thin torus

This is a LD radio-loud QSO with high, wavelength-independent degree of polarization, indicating an electron-scattered Type 1 spectrum and a completely obscured direct view of the nucleus. Unpolarized narrow lines of high equivalent width suggest a direct view of the NLR and an obscured continuum. The wavelength-independent polarization parallel to the radio jets indicates scattering in an optically-thin edge-on disk (Fig. 4(b) and (d)). While OI 287 is of high radio power, the extended radio features appear more like bridges than jets; in this respect it is more like IRAS 09104+4109, which has been suggested to have FR I radio structure.

4.5. 3CR 68.1, the Most Luminous 3CRR QSO

This z=1.2 AGN is special because it is the most luminous, most lobe-dominant QSO in the 3CRR catalog. Its optical-UV continuum is the reddest known – and it shows a highly polarized Type 1 spectrum, with degree of polarization increasing to $\sim$10% in the UV. This is interpreted in terms of a highly reddened direct spectrum, combined with a reddened scattered spectrum. Like OI 287, 3CR 68.1 shows strong associated absorption, which can be understood as the result of light from the center passing through absorbing clouds associated with the thinner regions of the torus (Fig. 2).

4.6. IRAS 13349+2438, a RQQ

This is the archetype of highly-polarized radio-quiet QSOs. It was the first QSO to be discovered in the mid infrared (12μm– 100μm) by IRAS. In the optical-UV it shows a strong, but reddened, Type 1 spectrum (z = 0.10), with extremely weak NLR emission. Its continuum and broad lines are increasingly polarized towards the UV, up to 10%, and its polarization (**E**-vector) is aligned with the major axis of a galaxy disk visible in the near IR. The explanation is in terms of a combination of a direct spectrum partially obscured by a dusty torus, and a much less-reddened (polarized) scattered spectrum. X-ray variability suggests a direct view to the center, but surprisingly, in view of the optical reddening, IRAS 13349+2438 is strong in soft X-rays (0.2keV – 0.6keV) with no sign of the expected cold absorption. This was one of the first examples of X-ray 'warm absorption'. The dust appears to be mixed with warm ionized gas that produces absorption only at higher photon energies, e.g., O VII and O VIII edges at $\sim$0.7 keV.

4.7. IRAS 07598+6508, a BAL QSO

Another IRAS-discovered radio-quiet QSO, IRAS 07598+6508, at z=0.15, was found first to have high polarization, leading to the discovery of extremely strong blue-shifted broad absorption lines (BALs) in the UV. Spectropolarimetry showed a polarized continuum and unpolarized broad emission lines, unlike the QSO 2s and Seyfert 2s investigated so far. This was the first object for which an increased degree of polarization was seen in an absorption line – indicating *decreased* dilution of a polarized continuum by an unpolarized absorbed

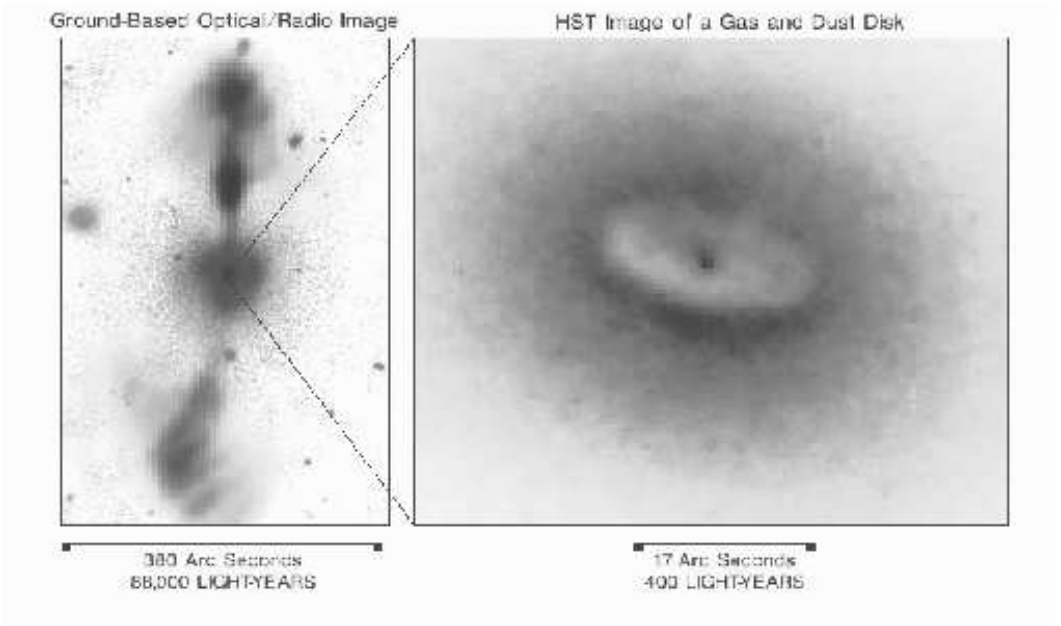

Figure 5. Left: The classic FR I radio source, 3C 270, showing the radio nucleus and ∼16 Kpc-long jets superposed on a ground-based optical image of the associated galaxy, NGC 4261. Right: The HST optical image of the nuclear regions of NGC 4261, showing the increasing stellar surface brightness towards the bright, unresolved nucleus, blocked by a dusty disk (shown lighter). The jets are almost aligned with the disk axis. NGC 4261 is a LINER galaxy (Low Ionization Nuclear Emission-line Region), with dynamical evidence suggesting a supermassive black hole (Ferrarese et al. 1996). Image from http://oposite.stsci.edu/pubinfo/Old.html. Observation by Jaffe et al. (1993). For updated optical images, see Jaffe et al. 1996, and especially Ferrarese et al. 1996). See also the NGC 7052 dust disk at http://oposite.stsci.edu/pubinfo/pr/1998/22/

continuum component. Because the broad emission lines are apparently not scattered, but part of the continuum is, the scatterers must lie nearer the QSO continuum source than the BLR, and be distinct from the absorption region. This is an important constraint on scattering geometry. Like other BAL QSOs it is not detected in X-rays, suggesting complete absorption by neutral gas with $N_H > 10^{23}$ cm^{-2}. IRAS 07598+6508 is also a 'super Fe II' emitter.

5. Dusty Torus Geometry: Statistical Relationships

5.1. Evidence for Dusty Tori, & Alignment

Dusty tori can be recognized by their absorbing effects in two ways: first, by their reddening and obscuration of light at high inclinations, and second, by dimming direct nuclear light, allowing the detection of a faint, scattered, polarized spectrum. The alignment of the polarization of a scattered Type 1 spectrum with

the radio jet is the strongest evidence for a nuclear dusty torus. Perpendicular or parallel alignment of the scattering polarization was recognized for a number of Seyfert and radio galaxies by Antonucci (1982, 1983), and interpreted as arising in the scattering geometries illustrated in Fig. 4 (see §4). The polarimetric evidence has been presented above by giving a few of many examples.

In nearby low luminosity AGN, where high spatial resolution is possible, flattened dusty regions or their outer 100 pc scale extensions can be recognized by direct imaging, either in absorption or infrared emission (see Fig. 5, and NGC 1068 above). Usually the disk axis is well aligned with the radio jets.

There is much evidence for dust in the NLR, and between the NLR and BLR, from differential reddening and differential polarization of the broad and narrow lines. Evidence for flattened dusty disks of high optical depth in the nuclear regions of low luminosity AGN was noted by de Zotti and Gaskell (1985). We note three nice statistical studies relating increasing extinction to increasing lobe dominance:
(i) Hill et al. (1996) sought to detect the obscured broad line region via observations of Paα in the near infrared where reddening effects are much smaller than the optical. They observed a complete sample of 3CR FR II AGNs, that is, AGN with radio luminosities in the QSO class. They found increasing reddening with decreasing core-dominance R (increasing inclination), consistent with a dusty torus model like that shown in Fig. 2.
(ii) Baker and collaborators (1995, 1997) have investigated a complete sample of low-frequency selected RL QSOs, showing the steepening of the optical continuum and reddening of the Balmer decrements with decreasing R.
(iii) Baker (1997) and earlier, Hes, Fosbury & Barthel (1994) have shown increasing narrow-line ratio [O II]λ3727/[O III]λ5007 with decreasing R, indicating the preferential obscuration of the higher-ionization [O III] emission that is expected to be produced closer to the nucleus.

Alignment of the central engine axis with the host galaxy is important for understanding Unified Schemes too, and for completeness we note an investigation by Schmitt et al. (1997) and an earlier one by Ulvestad and Wilson (1984), showing that the axis of small-scale radio structure in Seyfert galaxies appeared to avoid alignment with the host galaxy minor axis. A more recent analysis suggests that this is the result of observational selection (Nagar & Wilson 1999). They find that observations are consistent with a uniform distribution of radio jet direction relative to the galaxy axis.

Additional important evidence for the existence of dusty tori in all or most luminous AGN is the presence of the 3μm Bump in essentially all radio-loud QSOs and many radio-quiet QSOs, where the redshift is low enough to allow detection (§3.1). Models suggest that the near-infrared optical depths should depend on inclination (Ward 1995).

5.2. Ionization Cones

Gas and dust within the opening of the torus, and therefore illuminated by the central QSO, gives rise to the scattered broad line spectrum, as well as most of the NLR emission. The structure of these 'cones' is clearest for nearby Seyfert 2 galaxies, and more than a dozen are now known with quite clearly defined 'edges'. However, the emitting gas and dust is obviously clumpy, so the edges

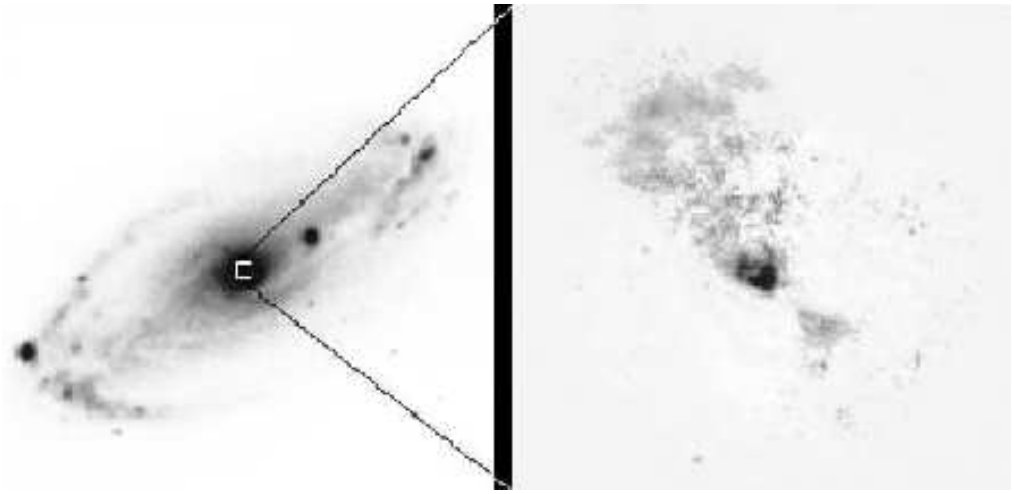

Figure 6. The biconical ionization structure in NGC 5728. An image in the light of the NLR [O III] $\lambda\lambda$4959, 5007 emission lines. Image from http://oposite.stsci.edu/pubinfo/Old.html. Observation by Wilson et al. (1993). For other examples, see Wilson & Tsvetanov (1994).

are often ill-defined. The first ionization cones were investigated by Pogge (1989) with arcsecond resolution. Several examples of bicones are seen (Fig. 6), but the cone facing away from the observer is often obscured. Opening angles range from 70° to 100°. The ionizing continuum deduced from the ionization state and density of the emitting gas is often brighter than the observed continuum. Unified schemes suggest that the dusty torus or its extensions blocks our view of the continuum. The dusty torus should be heated by this continuum, and for a given torus geometry one can predict the amount of re-radiated infrared emission. Storchi-Bergmann et al. (1992) confirm such predictions for 8 out of a small sample of 9 Seyfert 2s. A recent survey of early-type Seyfert galaxies (Nagar et al. 1999) and earlier work show that the axes of ionized emission are typically aligned within a few degrees of the inner radio jets. While some NLR emission is clearly excited by jet-related shocks (e.g., Capetti et al. 1996; Falcke et al. 1998), much of the ionized gas is not directly associated with the radio emission; there is ionized gas beyond the jet and the jets are rather more highly collimated than the ionized gas. Therefore, Wilson (1996) concludes, the radio plasma and ionizing photons are collimated by the same, or coplanar, disks or tori.

Another test is provided by a comparison of the optical and UV spectra of a sample of Seyfert 2 galaxies. Kinney et al. (1991) estimate the ionizing photons available from the observed UV continuum, concluding that in most cases there are insufficient to produce the observed emission line fluxes. Interestingly, the UV continua, while weak, have slopes indistinguishable from those of Seyfert 1 galaxies, consistent with the Seyfert 2 UV continuum being an electron-scattered Seyfert 1 continuum. Comparing a much larger sample of Seyfert 1 and Seyfert 2 AGN, Mulchaey et al. (1994) are able to show that, while the infrared continua, [O III] λ5007 NLR strengths, and the hard X-ray are similar in both classes, con-

sistent with isotropic emission, the UV and soft X-ray (0.2-4 keV) continua of Seyfert 2s are underluminous, consistent with line-of-sight absorption. In addition, they find that while the line emission and continuum fluxes are correlated in Seyfert 1s, consistent with the UV photons powering the lines emission, there is no such correlation for the Seyfert 2s, again consistent with our not seeing the ionizing continuum directly in Seyfert 2s.

There are similar results from calculations of the energy budget for a few higher luminosity radio-quiet QSOs [e.g., IRAS 09104+4109 (§4.7); IRAS 20460+1935 (Frogel et al. 1989)].

One can also check the opening angles derived by the above direct imaging results with those derived by comparing relative numbers of Type 2 and Type 1 AGNs, assuming that most of the Type 2 AGNs contain buried Type 1 nuclei. Opening angles derived from comparisons of Seyfert 1 and Seyfert 2 galaxies lie in the right ballpark – about 60° to 80° (e.g., Osterbrock & Shaw 1988). For RL AGNs, the comparison is easier because it is possible (with a lot of hard work) to select an orientation-independent sample by isotropic low-frequency radio emission. To avoid optical bias, the sample must be completely optically identified. This is how Barthel (1989), using the completely identified 3CRR sample (178 MHz – Laing, Riley & Longair 1983), derived the value $2\times \sim 45°$ used in §3.1. Willott, Rawlings & Blundell (this volume) use the much larger 7C sample selected at 151 MHz, and derive an opening angle of $\sim 120°$ for the most luminous QSOs. See their paper for a discussion of this difference.

5.3. Where are the QSO 2s?

QSO 2s are to 'normal' QSO 1s, as Seyfert 2s are to Seyfert 1s. It has sometimes been hotly claimed that QSO 2s don't exist, with the suggestion that high luminosity AGN have only small covering by a dusty torus.

Investigations of individual QSOs (e.g., §4) lead to a wide range in dust-covering fraction, and this raises the question of just how many luminous QSOs are we missing in samples selected by their optical-UV emission? The only way to address this question is to observe a complete sample of AGN selected by a property that is independent of orientation. Selection by low-frequency radio emission is the best method. The 3CRR sample selected at 178 MHz is excellent, and selection by FR II structure identifies those of QSO luminosities (Urry & Padovani 1995; Hill et al. 1996). This was the sample that led Barthel (1989) to propose that FR II radio galaxies were buried FR II QSOs. Thus, some NLRG and 3CR 68.1 (§4.5) are QSO 2s, and the BLRG and reddened QSOs (Smith & Spinrad 1980) are of intermediate inclination. See also Willott et al. (this volume).

Recent studies of reddening in RLQs are relevant. Webster et al. (1995) have found a significant number of red QSOs among a completely-identified sample of Parkes flat radio-spectrum sources. While some fraction of these might be expected to have a steep (and therefore red) IR-UV synchrotron component (Serjeant & Rawlings 1996, see §7) a significant fraction are probably dust reddened (Francis et al. 1997). Carilli et al. (1998) have found 4 of 5 red flat radio-spectrum QSOs with significant columns of neutral hydrogen – either the result of intervening absorbers or, in two cases, intrinsic to the QSO. This is interesting because, according to unified schemes, these flat-spectrum sources

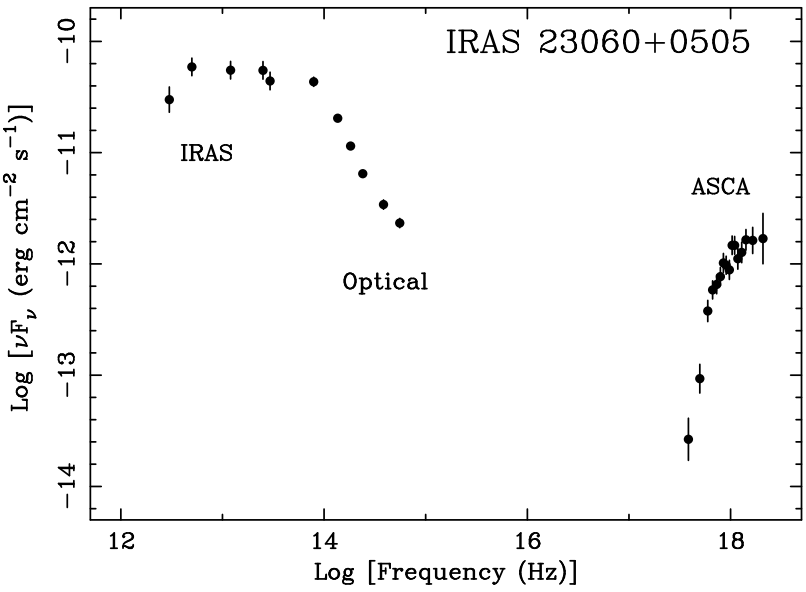

Figure 7. The observed spectral energy distribution of IRAS 23060+0505, a QSO 2 showing the reddened optical continuum and the X-ray absorption in the ASCA 2–10 keV band (the decrease in flux density towards soft X-ray energies). (Figure adapted from Brandt et al. 1997a.)

are CD QSOs and are therefore expected to be the least dust-reddened, so absorption (and reddening) is likely to be rather more for lobe-dominant sources where the line-of-sight passes closer to the plane of the dusty torus.

However the above studies apply only to RLQs.

The RQQs far outnumber the RLQs, so it is of interest to understand how Unified Schemes work for RQQs. The hard X-ray region ($>$ 10keV, Wilkes 1999, this volume) or the mid-infrared (e.g., Rush, Malkan & Spinoglio 1993) should be good wavelengths to select a sample because absorption by cold gas or dust, while not negligible, is much less. The X-ray data are not yet available. In the infrared one is overwhelmed by the huge numbers of galaxies, whose H II regions, excited by young stars, emit thermally in the infrared. A practical solution adopted by Low et al. (1988) and others is to select, in addition, by warm infrared colors. Neugebauer et al. (1986) had shown that warm infrared colors were an essentially unique signature of QSOs and Seyferts already discovered by optical techniques, so to find the same kinds of QSOs, independent of whether or not their optical-UV emission is covered by dust, Low et al. selected IRAS Type 1 spectra with $F_\nu(25\mu m)/F_\nu(60\mu m) > 1/4$. Using the same criteria, Wills & Hines (1997) defined a complete sample of extragalactic objects with L(IR)$> 10^{11.8}$L$\odot$(H_o = 50 km s^{-1} Mpc^{-1}), regardless of optical classification. Six objects (1/3 of the sample) had Type 2 spectra with Type 1 spectra revealed in polarized light, and are therefore QSO 2s. The spectral energy distribution of one of these is

shown in Fig. 7, where its steep optical UV spectrum, soft X-ray absorption, and recovery at harder X-ray energies, is illustrated. About 1/3 showed reddened Type 1 spectra in total and polarized light, providing evidence for a significant scattered-light contribution to a partially obscured direct view of the center. The remainder were less reddened, but only 3 of the sample had been found by conventional optical-UV selection techniques. When corrected for reddening the ratio of IR to optical flux is no different from typical optically-selected PG QSOs, so spectroscopically and with respect to their spectral energy distributions, these IRAS-selected luminous AGN appear to harbor 'normal' QSOs.

Two thirds of the sample AGN are either QSO 2s, objects of QSO luminosity dominated by Type 2 spectra but with buried QSO 1 nuclei, or QSOs without strong NLR emission, but with a reddened line-of-sight to the center, and a significant scattered Type 1 contribution – reddened QSO 1s. These would not have been discovered by conventional selection techniques. It is likely that even more-obscured luminous AGNs were missed by the IRAS color-selection, indicating that space densities of QSOs have been underestimated by a large factor.

6. Concluding Remarks

The present description of Unified Schemes has intentionally been simplified. Many aspects are the subject of active research. There is now a huge literature relevant to the subject – certainly over 1000 papers. Therefore I have selected some topics at the expense of others; I apologize for important papers not included.

Unification of the QSO majority, the most radio quiet, remains difficult without an indicator of inclination. One possibility is to search for ionization or scattering cones, but these may be small and faint. One might speculate whether beamed X-ray emission could be used as an orientation indicator for radio-quiet QSOs. The basis for this is the discovery of radio-weak BL Lac objects whose beamed radiation appears to be in the EUV to soft X-ray region (Stocke et al. 1985; Padovani & Giommi 1995). The minimum ingredients for a unification scheme are orientation and patchy dust, but there is good evidence for a richer and more interesting unified scheme based on an axisymmetric central engine surrounded by an obscuring dusty torus.

Some tantalizing links are suggested between the torus parameters and other AGN relationships. Covering by dense Fe II-rich gas, and outflowing BAL gas (§3.3), appear to be part of the 'Principal Component' relationships among X-ray continuum, broad line profiles, and the inverse relationship between Fe II strength and [O III] λ5007 (Wills et al., Aoki et al., this volume). Radio loudness appears to be another parameter linked to these Principal Component relationships and to properties of BAL outflows. Links between strong Fe II emission and dust abound in astrophysical situations, so, is there a relationship between covering by dense line-emitting gas and the dusty torus?

It has been suggested that the torus opening angle increases with luminosity. The X-ray slope and broad-line equivalent widths depend on luminosity (Korista et al., this volume). Broad line widths may also increase with luminosity.

We have yet to learn whether or how all these relationships may be linked.

Unification of diverse classes of AGN by changing aspect angle and extinction by dust is a reality, as foretold by Rowan-Robinson (1977). While most astronomers would like to sweep it under the rug, the complicated subject of dust must be confronted (e.g., Masci 1998). Not only does external dust absorb, scatter and emit thermal radiation, it affects the energy balance and chemistry of absorption and emission line regions. Most surveys for AGN are biased against dusty objects. This will change with new surveys in the radio, infrared and hard X-ray regimes. The lesson for cosmology is that the space density of QSOs has been underestimated, with important implications for their evolution and contribution to the cosmic background.

With increasing evidence for supermassive black holes in many galaxies, even those with little activity, it is clear from the space density and luminosity functions of galaxies and QSOs that QSOs are a phenomenon common to perhaps all massive galaxies, even if short-lived and intermittent. Therefore, what we learn about active galaxies and QSOs is relevant to the evolution of all galaxies, and to cosmology.

7. Additional References

Here I expand upon the references given in the above sections, with brief remarks.
General AGN Texts: Osterbrock 1989, Peterson 1997, Robson 1996, Krolik 1999, Weedman 1986, Longair 1981, Miller 1985, Burke & Graham-Smith 1997.
Radio-loud AGN Unification: Blandford & Rees 1978 (the classic paper on ideas behind present Unified Schemes) Vermeulen & Cohen 1994 (superluminal motion) Ghisellini et al. 1993 (statistics relating radio, optical & X-ray observations for several classes of AGN) Kellermann & Owen 1988 (general review of extragalactic radio sources at a basic level) Orr & Browne 1982 (RL QSO CD vs. LD statistics) Hughes, P. A. 1991 (Good theory and observation text) Browne & Perley 1986 (halos of CD sources) O'Dea, C. 1998 (Gigahertz Peaked Spectrum sources - a review) Urry (1999) (The FR I–FR II break).
Unification of FR II AGNs: Tadhunter, Dickson & Shaw 1996, Cimatti et al. 1998 (polarimetry of BLRG and reddened QSOs) Sanders et al. 1989, Barvainis 1987 (3 μm Bump) Shastri et al. 1993 (X-ray spectrum and core-dominance) Wills & Browne 1986, Vestergaard 1998 (broad-line width vs. core-dominance).
FR 1 AGN & BL Lac Objects: Ulrich et al. 1984, Stickel et al. 1993, Vermeulen et al. 1995, Corbett et al. 1996 (broad lines in BL Lac objects).
Seyfert galaxy unification: Tran 1995 (spectropolarimetry), Veilleux, Goodrich & Hill 1997 (near IR spectroscopy). Heisler, Lumsden & Bailey 1997 (even scattered light obscured at highest inclinations).
Radio-quiet QSOs: Arav, Shlosman & Weymann (eds) 1997, Korista et al. 1993, Glenn et al. 1994 (BAL QSOs, multiple light paths).
NGC 1068: Antonucci & Miller 1985, Bailey et al. 1988, Young et al. 1995 (spectropolarimetry) Roy et al. 1998 (absorbed radio nucleus) Bock et al. 1998 (IR imaging) Capetti et al. 1995 (polarization imaging) Greenhill, L. 1996 (VLBI H_2O maser) Matt et al. 1997 (hard X-ray spectrum) Gallimore, Baum, & O'Dea 1995 (pc-scale thermal emission from the torus).
NGC 4258: Miyoshi et al. 1995, Moran et al. 1995 (H_2O maser) Wilkes et al. 1995 (spectropolarimetry).

IRAS 09104+4109: Kleinmann et al. 1988 (discovery and spectra) Hines & Wills 1993, Hines et al. 1999 (spectropolarimetry and imaging) Crawford & Vanderreist 1996 (emission line imaging, X-ray).
OI 287: Ulvestad & Antonucci 1988 (radio structure) Rudy & Schmidt 1988, Miller & Goodrich 1988 (polarization) Antonucci, Kinney & Hurt 1993 (UV spectra).
3C 68.1: Brotherton et al. 1998.
IRAS 13349+2438: Beichmann et al. 1986 (discovery) Wills et al. 1992b, (spectroscopy, polarimetry) Brandt et al. 1997b (X-ray ionized absorption).
IRAS 07598+6508: Lawrence et al. 1988, Lipari 1994, Kwan et al. 1995 (strong Fe II emission) Hines & Wills 1995 (spectropolarimetry).
The dusty torus: Lawrence & Elvis 1982 (perhaps the first paper to suggest that Type 2 spectra were Type 1 spectra with absorbed broad line emission and absorbed soft X-rays), Ward 1995 (The Oxford Torus Workshop).
QSO 2s: Fugmann 1988, Impey, Lawrence & Tapia 1991, Wills 1991, Wills et al. 1992a (IR-optical synchrotron continuum).

Acknowledgments. I thank Jack Baldwin, Mike Brotherton and Derek Wills for many helpful comments. I am very grateful for the work of the staffs of the NASA Astrophysics Data System, the Eprint Astrophysics Archives, and the NASA Extragalactic Database, without whom this review would have been impossible. B.J.W. is supported by NASA through LTSA grant number NAG5-3431 and grant number GO-06781 from the Space Telescope Science Institute, which is operated by the Association of Universities for Research in Astronomy, Inc., under NASA contract NAS5-26555.

References

Antonucci, R. R. J. 1982 Nature, 299, 605

Antonucci, R. R. J. 1983 Nature, 303, 158

Antonucci, R. R. J. 1993, ARA&A, 31, 473

Antonucci, R. R. J., & Miller, J. S. 1985, ApJ, 297, 476

Antonucci, R. R. J., Kinney, A. L., & Hurt, T. 1993, ApJ, 414, 506

Antonucci, R. R. J., Hurt, T., & Miller, J. S. 1994, ApJ, 430, 210

Antonucci, R. R. J., & Ulvestad, J. S. 1985, ApJ, 294, 158

Arav, N., Shlosman, I., & Weymann, R. A. (eds.) 1997, Mass Ejection from AGN (San Francisco: ASP)

Bailey, J. A., Axon, D. J., Hough, J. H., Ward, M. J., McLean, I., Heathcote, S. R. 1988, MNRAS, 234, 899

Baker, J. C. 1997, MNRAS, 286, 23

Baker, J. C., & Hunstead, R. W. 1995, ApJ, 452, 95

Baker, J. C., Hunstead, R. W., & Brinkmann, W. 1995, MNRAS, 277, 553

Barthel, P. D. 1989, ApJ, 336, 606

Barvainis, R. 1987, ApJ, 320, 537

Becker, R. H., White, R. L., Helfand, D. J. 1995, ApJ, 450, 559

Beichman, C. A., Soifer, B. T., Helou, G., Chester, T. J., Neugebauer, G., Gillett, F. C., & Low, F. J. 1986, ApJ, 308, 1

Blandford, R. & Rees, M. 1978, in Pittsburgh Conference on BL Lac Objects, ed. A. M. Wolfe (Pittsburgh: University of Pittsburgh), 328

Blundell, K. M., & Beasley, A. J. 1998a, MNRAS, 299, 165

Blundell, K. M., & Beasley, A. J. 1998b, BAAS, Meeting No. 193, 110.04.

Bock, J. J., Marsh, K. A., Ressler, M. E., Werner, M. W. 1998, ApJ, 504, 5

Boroson, T. A., & Meyers, K. A. 1992, ApJ, 397, 442

Brandt, W. N., Fabian, A. C., Takahashi, K., Fujimoto, R., Yamashita, A., Inoue, H., Ogasaka, Y. 1997a, MNRAS, 290, 617

Brandt, W. N., Mathur, S., Reynolds, C. S., & Elvis, M. 1997b, MNRAS, 292, 407

Bridle, A. H., Hough, D. H., Lonsdale, C. J., Burns, J. O., Laing, R. A. 1994, AJ, 108, 766

Brotherton, M. S., Wills, B. J., Dey, A., Van Breugel, W., & Antonucci, R. R. J. 1998, ApJ, 501, 110

Browne, I. W. A. 1987, in Superluminal Radio Sources, eds. J. A. Zensus, & T. J. Pearson (Cambridge: CUP), 129

Browne, I. W. A., & Perley, R. A. 1986, MNRAS, 222, 149

Burke, B. F., & Graham-Smith, F. 1997, An Introduction to Radio Astronomy (Cambridge: CUP)

Capetti, A., Macchetto, F., Axon, D. J., Sparks, W. B., & Boksenberg, A. 1995, ApJ, 452, L87

Capetti, A., Axon, D. J., Macchetto, F., Sparks, W. B., Boksenberg, A. 1996, ApJ, 469, 554

Carilli, C. L., Menten, K. M., Reid, M. J., Rupen, M. P., & Yun, M. S. 1998, ApJ, 494, 175

Chary, R. & Becklin, E. E. 1997 ApJ, 485, 75

Cimatti, A., Di Serego Alighieri, S., Vernet, J., Cohen, M., & Fosbury, R. A. E. 1998, ApJ, 499, 21

Cohen, M. H. & Unwin, S. C. 1982, Proc. IAU Symposium No. 97, "Extragalactic Radio Sources", eds. D. S. Heeschen & C. M. Wade (Reidel: Dordrecht), 345

Corbett, E. A., Robinson, A., Axon, D. J., Hough, J. H., Jeffries, R. D., Thurston, M. R., Young, S. 1996, MNRAS, 281, 737

Crawford, C. S., & Vanderreist, C. 1996, MNRAS, 283, 1003

De Zotti, G., & Gaskell, C. M. 1985, A&A, 147, 1

Dennett-Thorpe, J., Bridle, A. H., Scheuer, P. A. G., Laing, R. A., Leahy, J. P. 1997, MNRAS, 289, 753

Falcke, H., Gopal-Krishna, & Biermann, P. L. 1995, A&A, 298, 395

Falcke, H., Wilson, A.S., & Ho, L.C. 1997, Proc. Conf. Relativistic Jets in AGNs, 13

Falcke, H., Patnaik, A. R., Sherwood, W. 1996a, ApJ, 473, 13

Falcke, H., Sherwood, W., Patnaik, A. R. 1996b, ApJ, 471, 106

Falcke, H., Wilson, A. S., Simpson, C. 1998, ApJ, 502, 199

Fanaroff B. L., & Riley, J. M. 1974, MNRAS, 167, 31P

Ferrarese, L., Ford, H. C., & Jaffe, W. 1996, ApJ, 470, 444

Francis, P.J., Webster, R. L., Masci, F. J., Drinkwater, M. J., Peterson, B. A. 1997, in Emission Lines in Active Galaxies: New Methods & Techniques, ed B. M. Paterson, F.-Z. Cheng, & A. S. Wilson (San Francisco: ASP), 130

Frogel, J. A., Gillett, F. C., Terndrup, D. M., & Vader, J. P. 1989, ApJ, 343, 672

Fugmann, W. 1988, A&A, 205, 86

Gallimore, J. F., Baum, S. A., & O'Dea, C. P. 1995, Nature, 388, 852

Ghisellini, G., Padovani, P., Celotti, A., Maraschi, L. 1993, ApJ, 407, 65

Giovannini, G., Arbizzani, E., Feretti, L., Venturi, T., Cotton, W. D., Lara, L., & Taylor, G. B. 1998, IAU Colloquium 164: Radio Emission from Galactic & Extragalactic Compact Sources, ASP Conference Ser. 144, eds. Zensus, J.A., Taylor, G.B., & Wrobel, J.M. (ASP: San Francisco), 85

Glenn, J., Schmidt, G. D., & Foltz, C. B. 1994, ApJ, 434, 47

Gopal-Krishna, Kulkarni, V. K., Wiita, P. J. 1996, ApJ, 463, 1

Grandi, S. A. & Osterbrock, D. E. 1978, ApJ, 220, 783

Green, P.J., & Mathur, S. 1996, ApJ, 462, 637

Greenhill, L. 1996, ApJ, 472, 21

Heisler, C. A., Lumsden, S. L., & Bailey, J. A. 1997, Nature, 385, 700

Hes, R., Fosbury, R. A. E., & Barthel, P. D. 1994, in The First Stromlo Symposium: The Physics of Active Galaxies, ASP Conference Ser. 54, eds. G. V. Bicknell, M. A. Dopita, & P. J. Quinn (ASP: San Francisco), 367

Hill, G. J., Goodrich, R. W., & DePoy, D. L. 1996, ApJ, 462, 163

Hines, D. C., Schmidt, G., Wills, B. J., Smith, P. S. & Sowinski, G. 1999, ApJ, 512, 000

Hines, D. C., & Wills, B. J. 1993, ApJ, 415, 82

Hines, D. C., & Wills, B. J. 1995, ApJ, 448, 69

Hooper, E. J., Impey, C. D., Foltz, C. B., Hewett, P. C. 1995, ApJ, 445, 62

Hough, D. H., & Readhead, A. C. S. 1989, AJ, 98, 1208

Hughes, P. A. (ed.) 1991, Beams & Jets in Astrophysics (Cambridge: CUP)

Impey, C. D., Lawrence, C. R., & Tapia, S. 1991, ApJ, 375, 461

Jaffe, W., Ford, H. C., Ferrarese, L., van den Bosch, F., & O'Connell, R. W. 1993, Nature, 364, 213

— 1996, ApJ, 460, 214

Jones, D.L. & Wehrle, A. E. 1998, IAU Colloquium 164: Radio Emission from Galactic & Extragalactic Compact Sources, ASP Conference Ser. 144, eds. Zensus, J.A., Taylor, G.B., & Wrobel, J.M. (ASP: San Francisco), 63

Kellermann, K. I., & Owen, F. N. 1988, in Galactic & Extragalactic Radio Astronomy, second edition, eds. K. I. Kellermann, & G. L. Verschuur (New York: Springer-Verlag), 563

Kellermann, K. I., Sramek, R. A., Schmidt, M., Green, R. F., Shaffer, D. B. 1994, AJ, 108, 1163

Kellermann, K. I., Vermeulen, R. C., Zensus, J. A., & Cohen, M. H. 1998, AJ, 115, 1295

Kinney, A. L., Antonucci, R. R. J., Ward, M. J., Wilson, A. S., Whittle, M. 1991, ApJ, 377, 100

Kleinmann, S. G., Hamilton, D., Keel, W. C., Wynn-Williams, C. G., Eales, S. A., Becklin, E. E., Kuntz, K. D. 1988, ApJ, 328, 161

Korista, K. T., Voit, G. M., Morris, S. L., & Weymann, R. J. 1993, ApJS, 88,357

Krolik, J. H. 1999, Active Galactic Nuclei (Princeton: Princeton University Press)

Kukula, M. J., Dunlop, J. S., Hughes, D. H., & Rawlings, S. 1998, MNRAS, 297, 366

Kwan, J., Cheng, F.-Z., Fang, L.-Z., Zheng, W., Ge, J. 1995, ApJ, 440, 628

Laing, R.A., Riley, J.M., & Longair, M.S. 1983, MNRAS, 204, 151

Lara, L., Márquez, I, Cotton, W. D., Feretti, L., Giovannini, G., Marcaide, J. M., & Venturi, T. 1998, astro-ph/9812254

Lawrence, A., & Elvis, M. 1982, ApJ, 256, 410

Lawrence, A. et al. 1988, MNRAS, 235, 261

Leahy, J. P., et al. 1997, MNRAS, 291, 20

Lind, K. R., & Blandford, R. D. 1985, ApJ, 295, 358

Lipari, S. 1994, ApJ, 436, 102

Longair, M. S. 1981, High Energy Astrophysics (Cambridge: CUP)

Low, F. J.,Cutri, R. M., Huchra, J. P., Kleinmann, S. G. 1988, ApJ, 327, 41

Malkan, M. A. & Sargent, W. L. W. 1983, ApJ, 254, 22

Masci, F. J. 1998, PASA, 15, 299

Matt, G., et al. 1997, A&A, 325, L13

Miller, J. S., & Antonucci, R. R. J. 1983, ApJ, 271, 7

Miller, J. S., & Goodrich, R. W. 1988, ApJ, 331, 332

Miller, J. S., Goodrich, R. W., & Mathews, W. G. 1991, ApJ, 378, 47

Miyoshi, M., Moran, J. M., Herrnstein, J. R., Greenhill, L. J., Nakai, N., Diamond, P. J., & Inoue, M. 1995, Nature, 373, 127

Morganti, R., Parma, P., Capetti, A., Fanti, R., De Ruiter, H.R., 1997, A&A, 326, 919

Mulchaey, J. S., et al. 1994, ApJ, 436, 586

Mushotzky, R. F. 1997, in Mass Ejection from AGN, ASP Conference Ser. 128, eds. N. Arav, I. Shlosman, & R. J. Weymann (ASP: San Francisco), 141

Moran, J. M., Greenhill, L. J., Herrnstein, J. R., Diamond, P. J., Miyoshi, M., Nakai, N., & Inoue, M. 1995, Proc. Natl. Acad. Sci., 92, 11427

Morganti, R., Parma, P., Capetti, A., Fanti, R. & de Ruiter, H. R. 1997, å, 326, 919

Nagar, N. M., & Wilson, A. S. 1999, ApJ, 516, No. 1

Nagar, N. M., Wilson, A. S., Mulchaey, J. S., & Gallimore, J. F. 1999, ApJS, 120, No. 2

Neeser, M. J., Eales, S. A., Law-Green, J. D., Leahy, J. P., Rawlings, S. 1995, ApJ, 451, 76

Neugebauer, G., Soifer, B. T., Miley, G. K., & Clegg, P.E. 1986, ApJ, 308, 815

O'Dea, C. P. 1998, PASP, 110, 493

Orr, M. J. L., & Browne, I. W. A. 1982, MNRAS, 200, 1067

Osterbrock, D. E. 1989, Astrophysics of Gaseous Nebulae & Active Galactic Nuclei (Mill Valley: University Science Books)

Osterbrock, D. E., & Shaw, R. A. 1988, ApJ, 327, 89

Owen, F. N., Ledlow, M. J., & Keel, W. C. 1996, AJ, 111, 53

Packham, C., Young, S., Hough, J. H., Axon, D. J., Bailey, J. A. 1997, MNRAS, 288, 375

Padovani, P., & Giommi, P. 1995, ApJ, 444, 567

Penston, M. V., & Perez, E. 1984, MNRAS, 211, 33P

Peterson, B. M. 1997, An Introduction to Active Galactic Nuclei (Cambridge:CUP)

Pogge, R. W. 1988, ApJ, 328, 519

Pogge, R. W. 1989, ApJ, 345, 730

Robson, I. Active Galactic Nuclei (Chichester: Wiley-Praxis)

Roy, A. L., Colbert, E. J. M., Wilson, A. S., Ulvestad, J. S. 1998, ApJ, 504, 147

Rudy, R. J. & Schmidt, G. D. 1988, ApJ, 331, 325

Rush, B., Malkan, M. A., & Spinoglio, L. 1993, ApJS, 89, 1

Sanders, D. B., Phinney, E. S., Neugebauer, G., Soifer, B. T., Matthews, K. 1989, ApJ, 347, 29

Schmitt, H. R., Kinney, A. L., Storchi-Bergmann, T., & Antonucci, R. R. 1997, ApJ, 477, 623

Shastri, P., Wilkes, B. J., Elvis, M., McDowell, J. 1993, ApJ, 410, 29

Shields, G. A. 1978, Nature, 272, 706

Smith, H. E., & Spinrad, H. 1980, ApJ, 236, 419

Stickel, M, Fried, J. W., & Kühr, H. 1993, A&AS, 98, 393

Stocke, J. T., Liebert, J., Schmidt, G, Gioia, I. M., Maccacaro, T., Schild, R. E., Maccagni, D., & Arp, H. C. 1985, ApJ, 298, 619

Storchi-Bergmann, T., Mulchaey, J. S., & Wilson, A. S. 1992, ApJ, 395, 73

Tadhunter, C. N., Dickson, R. C. & Shaw, M. A. 1996 MNRAS, 281, 591

Tran, H. D. 1995, ApJ, 440, 597

Tran, H. D., Brotherton, M. S., Stanford, S. A., van Breugel, W., Dey, A., Stern, D., & Antonucci, R. R. J. 1999, ApJ, in press

Trotter, A. S., Greenhill, L. J., Moran, J. M., Reid, M. J., Irwin, J. A., & Lo, K.-Y. 1998, ApJ, 495, 740

Turnshek, D. A., Monier, E. M., Sirola, C. J., & Espey, B. R. 1997, ApJ, 476, 40

Ulrich, M. H., Hackney, K. R. H., Hackney, R. L., & Kondo, Y. 1984, ApJ, 276, 466

Ulvestad, J. S., & Antonucci, R. R. J. 1988, ApJ, 328, 569

Ulvestad, J. S., & Wilson, A. S. 1984, ApJ, 285, 439

Urry, C. M. 1999, in The BL Lac Phenomenon (Turku, Finland)

Urry, C. M., & Padovani, P. 1995, PASP, 107, 803

Veilleux, S., Goodrich, R. W., Hill, G. J. 1997, ApJ, 477, 631

Vermeulen, R. C., & Cohen, M. H. 1994, ApJ, 430, 467

Vermeulen, R. C., et al. 1995, ApJ, 452, 15

Vestergaard, M. 1998, PhD thesis, Univ. of Copenhagen

Ward, M. J. (ed.) 1994, Oxford Astrophysics Workshop on Evidence for the Torus

Wardle, J. F. C., & Aaron, S. E. 1997, MNRAS, 286, 425

Webster, R. L., Francis, P. J., Peterson, B. A., Drinkwater, M. J., & Masci, F. J. 1995, Nature, 375, 469

Weedman, D. W. 1986, Quasar Astronomy (Cambridge: CUP)

Weymann, R. J., Morris, S. L., Foltz, C. B., Hewett, P. C. 1991, ApJ, 373, 23

Weymann, R. J. 1997, in Mass Ejection from AGN, ASP Conference Ser. 128, eds. N. Arav, I. Shlosman, & R. J. Weymann (ASP: San Francisco), 3

Wilkes, B. J., Schmidt, G. D., Smith, P. S., Mathur, S., & McLeod, K. K. 1995, ApJ, 455, L13

Wills, B. J. 1991, in Variability of Active Galactic Nuclei, eds. H. R. Miller & P. J. Wiita (Cambridge: CUP), 87

Wills, B. J., & Browne, I. W. A. 1996 ApJ, 302, 56

Wills, B. J., & Hines, D. C., in Mass Ejection from AGN, ASP Conference Ser. 128, eds. N. Arav, I. Shlosman, & R. J. Weymann (ASP: San Francisco), 99

Wills, B. J., Wills, D., Breger, M., Antonucci, R. R. J., & Barvainis, R. 1992a, ApJ, 398, 454

Wills, B. J., Wills, D., Evans, N. J., Natta, A., Thompson, K. L., & Breger, M. 1992b, ApJ, 400, 96

Wilson, A. S. 1996, Vistas in Astronomy, 40, 63

Wilson, A. S., & Tsvetanov, Z. I. 1994, AJ, 107, 1227

Wilson, A. S., Braatz, J. A., Heckman, T. M., Krolik, J. H., & Miley, G. K. 1993, ApJ, 419, 61

White, R. L. et al. 1999, AJ, in press

Young, S., Hough, J. H., Axon, D. J., Bailey, J. A., Ward, M. J. 1995, MNRAS, 272, 513